Published in final edited form as:
J Musculoskelet Neuronal Interact. 2008 ; 8(3): 227–238.

Asymmetric bone adaptations to soleus mechanical loading after spinal cord injury

S. Dudley-Javoroski and **R.K. Shields**
Graduate Program in Physical Therapy and Rehabilitation Science, The University of Iowa, Iowa City, IA, USA

Abstract

The purpose of this report is to examine longitudinal bone mineral density (BMD) changes in individuals with spinal cord injury (SCI) who began unilateral soleus electrical stimulation early after injury. Twelve men with SCI and seven without SCI underwent peripheral quantitative computed tomography assessment of distal tibia BMD. After 4.5 to 6 years of training, average trained limb BMD was 27.5% higher than untrained limb BMD. The training effect was more pronounced in the central core of the tibia cross-section (40.5% between-limb difference). No between-limb difference emerged in the anterior half of the tibia (19.2 mg/cm^3 difference, p>0.05). A robust between-limb difference emerged in the posterior half of the tibia (76.1 mg/cm^3 difference, p=0.0439). The posterior tibia BMD of one subject remained within the range of non-SCI values for 3.8 years post-SCI. The results support that the constrained orientation of soleus mechanical loads, administered over several years, elicited bone-sparing effects in the posterior tibia. This study provides a demonstration of the bone-protective potential of a carefully controlled dose of mechanical load. The specific orientation of applied mechanical loads may strongly influence the manifestation of BMD adaptations in humans with SCI.

Keywords

Peripheral Quantitative Computed Tomography; Electrical Stimulation; Compression; Tension

Introduction

The loss of normal physiologic loading after spinal cord injury (SCI) predisposes people with paralysis to rapid, severe bone mineral density (BMD) decline in paralyzed extremities. Because muscular contractions are the largest contributor of loads to bone[1], the restoration of muscular loads is a logical prospective strategy for the preservation of BMD after SCI. Over the years, it has become clear that not all forms of artificial muscular loading (induced via electrical stimulation) possess the same potential efficacy[2]. In studies that failed to demonstrate a bone anabolic response to muscular loading, numerous uncertainties remain about the magnitude, frequency, duration, and subject compliance with the tested intervention[3-10]. Such difficulty in establishing the optimal dose for bone-protective interventions limits our ability to judge the merits of mechanical loading for preventing post-SCI bone loss[11].

The interpretation of mechanical loading protocols is made clearer when the dose of the applied intervention is carefully monitored and controlled. We recently demonstrated that long-term

Corresponding author: Richard K. Shields, Ph.D., PT, FAPTA, Graduate Program in Physical Therapy and Rehabilitation Science, The University of Iowa, 1-252 Medical Education Building, Iowa City, IA 52242-1190,USA E-mail: richard-shields@uiowa.edu.

The authors have no conflict of interest.

electrically-elicited soleus contractions delivered sufficient loads to the tibia to attenuate the post-SCI decline in trabecular BMD[12]. Soleus loads approximated 1.5 times body weight and were performed ~8,000 times a month over the study. Because subjects performed most training bouts at home, we tracked subject compliance via data-monitoring software housed in the muscle stimulator (rather than with logbooks, phone calls, or other traditional compliance-monitoring methods). This level of surveillance allowed us to intervene when compliance fluctuated and it facilitated our understanding of long-term training effects. We now understand the approximate dose of stress necessary to elicit the observed training effect (31% higher BMD in trained limbs than in untrained limbs[12]).

To simplify the design of the soleus biomechanical model, we conceptualized that soleus mechanical loads would uniformly load the entire tibia cross-section. However, we know that while bone is a rigid material, it should bend when exposed to soleus muscle contraction forces[13]. We suspected that asymmetric training effects occurred in the tibiae of individuals involved with long-term soleus training. If this were indeed the case, we would gain an important insight into whether single-muscle electrical stimulation protocols should be superseded by multiple-muscle protocols designed to more symmetrically load the bone. Secondly, the hormonal, vascular, and neural factors known to contribute to post-SCI bone loss[14-21] likely influence the posterior and anterior regions of the tibia in a relatively uniform manner. Accordingly, an asymmetric training effect due to mechanical loading would shed light on the complex interplay of the many factors that precipitate post-SCI bone loss.

The purpose of this study is to examine the symmetry of longitudinal BMD changes in men who began a unilateral soleus electrical stimulation protocol early after SCI and who continued loading the tibia in this manner for up to 6 years. We compare the magnitude of the training effect to people with sub-acute SCI, chronic SCI, and people without SCI. In addition, we present a new method to inspect the tibia cross-section for asymmetrical training effects due to muscle loading. We hypothesize that BMD loss will be asymmetric in accordance with the stresses associated with soleus muscle activation.

Methods

Subjects

Twelve individuals with SCI underwent peripheral quantitative computed tomography (pQCT) assessment of the distal tibia (Table 1). All subjects presented with motor complete (ASIA A or B[22]) SCI. The protocol was approved by the University of Iowa Human Subjects Institutional Review Board and all subjects provided written informed consent before participating. An additional seven individuals without SCI underwent pQCT assessment as the control cohort. Exclusion criteria for all subjects were a history of bone pathology (i.e., bone metabolic disease, cancer, etc.), thyroid disorder, previous fracture at the scan site, and medications known to affect bone metabolism. Subjects with SCI were excluded if they experienced frequent spasms that would likely induce pQCT scan artifacts.

The non-SCI and chronic SCI subjects appeared in a previous report[23]. For the current report, their data are presented using new analysis procedures that offer enhanced information about the spatial features of the tibia cross-section. Data from the non-SCI subjects and the chronic SCI subjects provide “bookend” values to which the longitudinal data can be compared. Data from subject SCI 1 recently appeared in a case report[13].

Longitudinal data are provided by two cohorts of subjects with SCI of varying durations (Figure 1). First, three subjects (SCI 1, 2, and 3, Table 1) were enrolled in a unilateral soleus training program within our laboratory. Five additional subjects (SCI 4-8, Table 1) with acute or subacute SCI performed no soleus training.

The scan session time for both limbs (including time for transfers and positioning) was approximately 90 minutes. At his initial assessment, subject SCI 6 was still gaining medical stability and could not tolerate a long scan session. Only his left tibia was scanned on that date. Subject SCI 8 also elected to undergo unilateral assessment due to time constraints. All other scans were conducted bilaterally, and data from the two limbs can be compared in the figures (the two limbs for any given scan date share x-axis coordinates).

Training history and dose

Subjects SCI 1, 2, and 3 appeared in a previously published report of isometric soleus muscle electrical stimulation training[12]. The present report includes a new spatial partitioning analysis of these subjects' pQCT scans and an additional 2-3 years of data (Figure 2) regarding bone (tibia) adaptations to training. In brief, the subjects stimulate one soleus on 5 days per week using a home-based limb constraining system, stimulator and data logger. Unilateral stimulation provided a within-subject control that minimized the confounding influences inherent to recruiting a separate non-training control group (maturational, hormonal, and dietary differences, to name a few). During electrical stimulation training, the subject's knee was positioned at 90 degrees of flexion and the foot was tightly secured to a platform via straps over the knee. This limb constraint system prevented plantar flexion during soleus stimulation. Because the gastrocnemius muscle origin is proximal to the knee, placing the knee in 90 degrees of flexion minimized the torque that could be developed by the gastrocnemius[24]. The mechanical loads delivered to the tibia were predominantly generated by contraction of the soleus muscle.

The soleus was activated maximally (15 Hz) for 667 milliseconds every 2 seconds for 120 contractions. The data logger records the date, time, and number of stimulus pulses delivered to the muscle, enabling us to track subject compliance with the requested dose of loading. These subjects began home-based soleus training within the first 16 weeks post-SCI and have continued training for between 4.4 and 6 years. The subjects were requested to perform 10,000 soleus contractions per month and have successfully maintained over 80% compliance (8,000 contractions per month) with this prescribed loading dose throughout their training tenure. We previously determined that the dose of compressive load delivered to the distal tibia via this training method approximates 1.5 times body weight[12].

pQCT measurements

Scan procedure

pQCT measurements were performed with a Stratec XCT-2000 or 3000 densitometer (Stratec Medical, Pforzheim, Germany). Accuracy of this device is 2% (to the COMAC phantom); precision is +/−3 mg/cm^3 for trabecular bone and +/−9 mg/cm^3 for cortical bone[25]. This device is calibrated with respect to fat (fat density=0 mg/cm^3).

The tibiae were marked and measured according to our standard procedure[23]. Briefly, each subject placed one leg in a “figure-4” position (the lateral side of one foot resting on the contralateral knee). The investigators marked the most distal palpable tip of the medial malleolus and the most proximal edge of the medial tibial plateau with a fine-point pen. The investigators obtained tibia length by measuring between these marks, then repeated this procedure for the other limb. They then passed one of the subject's limbs through the pQCT gantry and secured the subject's foot onto a footplate. Using an inclinometer placed just distal to the tibial tuberosity, the investigators adjusted the vertical height of the footplate in order to bring the pitch of the shank to horizontal. A radiology technician performed a scout view of the talocrural joint and placed a reference line at the tibia endplate, bisecting the region of highest density at the lateral side of the distal tibia. Using this reference line, the scanner

obtained an image at 4% of tibia length (Figure 1). The voxel size was 0.4 mm^3, the scanner speed was 25 mm/s, and slice thickness was 2.2 mm.

Routine analysis procedures

The first post-scan analysis provided overall BMD values for the entire distal tibia cross-section. An investigator defined a region of interest that incorporated a small amount of soft tissue outside of the periosteal margin. A threshold algorithm removed voxels below 200 mg/cm^3, starting from the outer edge of the region of interest and moving inward. This removed all voxels corresponding to muscle and fat and defined the periosteal edge. (Our previous pQCT reports[12,23] used a variation of this method (a more complex iterative contour search), but we found that this strategy often failed to detect the periosteal border in subjects with very low BMD, such as those with chronic SCI. To preserve uniform analysis procedures for all subjects, we employed a simpler threshold approach in this report). Inside the periosteal border, densities higher than 400 mg/cm^3 were defined as cortical/subcortical bone and values lower than this threshold were defined as trabecular bone. A 3×3 voxel filter then proofed the image to detect pockets of high-density values. Voxels that had substantially higher BMD than the surrounding voxels were reassigned as subcortical bone and were excluded from further analysis. Trabecular BMD was obtained from the resulting image (a trabecular core with the cortical shell "peeled" away) (Figure 1). Because the cortical shell is very thin at 4% (and is therefore subject to the partial-volume effect[26]), we report only trabecular BMD for this site.

To facilitate comparison of our data with previously-reported values, we conducted a second analysis using a peel strategy commonly employed by other research groups[27,28]. As above, we delineated the periosteal contour using a 200 mg/cm^3 threshold. Next, we applied a "concentric peel" starting at the periosteal edge and ending when only 45% of the bone area remained (Figure 1). Trabecular BMD is reported for this central region of the tibia cross-section.

Anterior-posterior compartment analysis

In order to examine regional differences in tibia bone adaptation to soleus load, we devised a method to partition the tibia cross-section into anterior and posterior compartments. An investigator drew a line that touched the posterior surface of the tibia and the fibula. The investigator then drew a second line parallel to the first line, anchored at the most anterior voxel of the fibula. The posterior line was erased, leaving the line bisecting the tibia image (Figure 1). Beginning and ending where this line intersected the periosteum, the investigator traced a region of interest that adhered tightly to the posterior tibia periosteal border along a periosteal density zone corresponding to 153.4 mc/cm^3 (a maroon color that was easily discernible in the display palette). Again starting and ending at the periosteum, the investigator created a similar region of interest encompassing the anterior half of the tibia.

For both the anterior and posterior tibia regions of interest, we applied a threshold of −100 mg/cm^3 to define the "periosteal" border. This very low threshold eliminated no voxels from the region of interest; we thus analyzed all cortical, trabecular, and fat voxels in the image. By using a low threshold that retained marrow fat voxels, we forced the contour detection algorithm to follow the line bisecting the tibia, rather than seeking to follow (often sporadic) trabecular bone voxels. We continued to use a threshold of 400 mg/cm^3 and a 3×3 voxel filter in the next analysis step to exclude cortical and subcortical voxels, then obtained the trabecular density of each semicircular region of interest. We are therefore able to quantify the degree to which the trabecular lattice has been replaced by fatty marrow, even for subjects with extremely little surviving trabecular bone.

Repeatability of the partitioning protocol

The placement of the line bisecting the tibia required a degree of visual discernment by the investigator. We assessed the reproducibility of this procedure by placing the line of demarcation in a single image over two blinded trials. We measured the BMD difference between the two trials to determine the maximum BMD error associated with variations in line placement. We also determined the degree to which the endpoints of the line of demarcation differed between the two blinded trials (repeatability). We determined repeatability of line placement and BMD error due to line placement for the first and final scans of half of the SCI subjects (SCI 1 through SCI 6, Table 1).

Statistical procedures

We calculated Pearson Product Moment correlation coefficients, performed a paired t-test, and calculated the BMD percentage error to establish the repeatability of the tibia partitioning protocol. We used a two-way ANOVA to compare the BMD of the anterior and posterior partitions between and within subject cohorts. We also used one-way ANOVAs to determine whether the percentage difference between anterior and posterior BMD for the soleus training subjects differed from other subject cohorts. Significance was set at p=0.05.

Results

Repeatability of the partitioning protocol

Overall, a line endpoint could be placed within 0.349 (SE=0.034) summed mm from its previous blinded location (r=0.99). BMD did not differ between repeated line-placement trials (p>0.05, r=0.99). Therefore, the degree of line-placement error had a negligible effect on measured BMD. For both the anterior and posterior regions, mean absolute BMD difference between the first and second trials was 0.957 mg/cm^3. (SE=0.161 and 0.166 mg/cm^3 respectively, range=0.10 to 3.30 mg/cm^3). This equalled an average 0.537% error in BMD over repeated line placement trials. The worst-case BMD error (3.30 mg/cm^3) was equivalent to a 1.45% difference in BMD between trials.

Training effects

A representative example shows the BMD of the trained and untrained limbs of an individual with SCI (Figure 2). Trabecular BMD at the 4% tibia site for the non-SCI subjects averaged 255.2 (7.3) mg/cm^3 (Figure 3) and did not differ between left and right limbs (p=0.55). Data values for subjects scanned within the first year after SCI clustered around this value (range 190.7 (SCI 7) to 294.6 (SCI 8)). Three subjects scanned longitudinally showed a gradual BMD decline of up to 35% in the first 2.0 years post-SCI (SCI 4-6). Subjects with chronic SCI demonstrated the lowest average BMD; (101.3 mg/cm^3), which was equivalent to only 39.72% of the non-SCI BMD value.

For the soleus training cohort, trained limb BMD was higher than untrained limb BMD at all measurement points (Figure 2 and 3). The mean absolute between-limb difference for soleus trainers was 42.5 mg/cm^3 (range: 11.4 to 62.8 mg/cm^3), a 23.77% difference over all measurement times. As depicted in Figure 4, the soleus cohort between-limb training effect intensified with continued training history. At the most recent assessment, average trained limb BMD was 27.5% higher than untrained limb BMD for these subjects (Figure 3). This between-limb BMD difference was significantly higher for the soleus cohort than for the SCI subjects who did no soleus training (p=0.00013). Thus the between limb difference for the soleus cohort exceeded what would normally be anticipated in a sample of subjects with SCI, supporting a robust training effect upon tibia BMD.

The soleus training effect was even more pronounced when only the central 45 percentage of the trabecular envelope was considered (Figure 4). The soleus cohort trained limb average BMD exceeded untrained limb BMD by 58.2 (7.6) mg/cm^3, equivalent to a 35.4% difference. As before, the training effect of soleus loading intensified with training history, reaching a 40.4% between-limb difference in BMD at the most recent measurement.

Asymmetry of regional BMD

Trabecular BMD at the anterior tibia region for the non-SCI subjects averaged 247.6 (9.17) mg/cm^3 (Figure 5). Data values for subjects scanned within the first year after SCI clustered around this value (range 194.3 (SCI 7) to 287.6 (SCI 8)). Subjects scanned longitudinally showed a gradual decline in BMD. BMD for subjects with chronic SCI was 102.3 mg/cm^3, only 41.3% of the non-SCI BMD value ($p<0.0001$) (Table 2).

Trabecular BMD at the posterior tibia region for the non-SCI subjects averaged 272.7 (8.74) mg/cm3 (Figure 6). Data values for subjects scanned within the first year after SCI clustered around this value (range 181.6 (SCI 3) to 303.8 (SCI 8)). Subjects scanned longitudinally showed a gradual decline in BMD. BMD for subjects with chronic SCI was 98.5 mg/cm^3, only 36.1% of the non-SCI BMD value ($p<0.0001$) (Table 2).

For the non-SCI subjects and soleus training subjects, BMD of the posterior tibia region exceeded anterior region BMD ($p<0.05$) (Table 2). No statistically significant differences emerged between anterior and posterior BMD for the SCI subjects who did no training or for the chronic SCI subjects.

Asymmetry of training effect

Soleus training minimally preserved BMD in the anterior region of the tibia.

In most cases, the trained limb BMD exceeded untrained limb BMD, but the between-limb differences were small (−4.9 to 35.5 mg/cm^3, mean (SE)=19.2 (3.0)) (Figure 5). At the most recent assessment, trained limb anterior BMD differed neither from untrained limb anterior BMD nor from chronic SCI anterior BMD ($p>0.05$) (Table 2). Likewise, untrained limb anterior BMD at the final assessment did not differ significantly from the chronic SCI value ($p>0.05$) (Table 2).

In contrast, soleus training had a preservative effect upon BMD of the posterior region of the tibia (Figure 6). Absolute between-limb posterior BMD differences were large (22.8 to 114.1 mg/cm^3, mean (SE)=76.1 (7.2 mg/cm^3)), a nearly four-fold greater trained-versus-untrained difference than was observed in the anterior tibia region (Figure 5). At the most recent assessment, trained limb posterior BMD was significantly higher than untrained limb posterior BMD ($p=0.0439$), and more than double the chronic SCI value (64% difference, $p=0.002$) (Table 2). At this same measurement time, untrained limb posterior BMD did not significantly differ from the chronic SCI value ($p>0.05$). Non-SCI posterior tibia BMD (272.7 (8.74) mg/cm^3) exceeded the soleus group's final trained limb posterior BMD value by just 21.6%. Subject SCI 2 demonstrated particularly noteworthy preservation of posterior tibia BMD. At 3.8 years post-SCI, this subject's posterior BMD value (264.4 mg/cm^3) remained within the standard error for the non-SCI group posterior region BMD.

The asymmetrical training effect of long-term soleus electrical activation can best be observed by comparing adaptations in the anterior versus posterior compartments of individual limbs. Figure 7 shows the percentage absolute difference in posterior versus anterior BMD for the various subject cohorts at all measurement points. Right and left limb data are pooled for non-SCI, chronic SCI, and SCI non-trainer subject groups. In all limbs, except those which engaged in soleus training, BMD was fairly uniform across the tibia cross-section (posterior BMD was

8.9% to 14.1% higher than anterior BMD). In contrast, the trained limbs demonstrated 41.9 (4.6) percentage higher BMD in the posterior than the anterior tibia region. This finding suggests that mechanical factors, associated with stress exerted by the soleus muscle, were the major factor contributing to bone preservation after long-term SCI.

Discussion

In our previous report of soleus muscle stimulation training, BMD was 31% higher in the trained tibia after ~2.5 years of training[12]. At the end of that study, three subjects elected to continue the soleus training protocol. For all of these subjects, the bone-sparing effect of soleus loading persisted over two additional years of training, even to 6 years post-injury. We now observe what appears to be a more robust bone-sparing effect in the posterior aspect of the tibia. This recent observation lends support to the theory that the loss of mechanical load predominates as the mechanism contributing to bone loss after SCI. This finding has important implications for understanding the physiology of bone adaptation to loading in humans with paralysis. It may also bear upon the future translation of electrically-induced loading to maintain skeletal integrity in preparation for a cure after SCI. We determined that the asymmetric bone-sparing effect of soleus loading is considerable and that BMD of the posterior tibia region remained high in subjects who were 4 to 6 years post-SCI (Figure 2).

Longitudinal BMD decline

BMD values for the non-SCI cohort (~255 mg/cm^3) were commensurate with previous reports for this anatomic location[23,27]. As would be expected, initial BMD for subjects with subacute SCI differed little from this non-SCI value and appeared to be influenced by subject age (the oldest subacute SCI subject, SCI 7, had considerably lower BMD than the subacute SCI subjects in their 20s). BMD declined precipitously for subacute SCI subjects who were followed longitudinally. In the most extreme case, BMD for subject SCI 5 declined by 35% between 0.2 and 1.2 years post-SCI.

The age of SCI onset for the soleus training cohort ranged from 21 to 29 years (Table 1). It is thus reasonable to assume that their own subacute-phase BMD values would have fit within the range of values demonstrated by this study's subacute SCI subjects. The untrained limbs of the soleus cohort can offer a projection of the BMD decline the non-training SCI subjects will undergo in the future, culminating in a steady-state value between 3 and 8 years post-SCI[29]. The untrained limbs of subjects SCI 1 and SCI 3 (starting at 2.4 and 4.3 years post-SCI, respectively) appear to have reached a steady state value, commensurate with the steady state BMD timeline from previous reports[29].

We have assumed that the BMD values demonstrated by our subjects with chronic SCI are representative of the post-SCI steady state. Without longitudinal data for these subjects, this assumption requires additional support. To explore this further, we peeled the tibia image down to the central 45%, a method used in a previous report that explored the timing of the BMD steady state phase[29]. Mean peeled BMD for the chronic SCI subjects in the present study was 68.83 mg/cm^3 (Figure 4), a close match to previously published steady state values (66.1 mg/cm^3, [29]). It is therefore reasonable to assume that BMD of the SCI non-trainer subjects and the untrained limbs of soleus training subjects will eventually resemble the chronic SCI values.

Attenuation of BMD decline

Soleus training attenuated the longitudinal decline of BMD after SCI. After 4.5 to 6 years of training, trained limb BMD exceeded the untrained limb BMD (within-subject controls) by 27.5%, a similar training effect magnitude as observed in our previous report[12]. An additional two years of training maintained the relative difference in BMD between trained and untrained

limbs. The absolute BMD values for both limbs, however, continued to decline. While soleus training could therefore attenuate the normally occurring BMD decline after SCI, it did not arrest the decline entirely.

Our preferred manner of analyzing the pQCT images is somewhat conservative; we sample BMD from the entire trabecular envelope. However, we believe that bone loss after SCI may be most severe at the center of the tibia cross-section. At the 4% site, the marrow cavity is just beginning to form in the center of the tibia (Figure 1). When routine strains fall below a hypothetical "minimum effective strain for remodeling" (MESr)[30], bone mineral is removed primarily from bone surfaces that are in contact with marrow[31]. To examine BMD loss in this potentially vulnerable central region, we peeled the pQCT image down to 45% of the original area. Between-limb differences in the training cohort rose to 40.4% when analyzed in this manner. Thus in the region of the tibia cross-section presumed to be the most susceptible to disuse remodeling, the bone-sparing effect of the loading protocol was most pronounced.

Bone adaptation can occur in two ways; via remodeling, as described above, and via modeling, which occurs primarily at the periosteal and endosteal surfaces of the diaphysis. Modeling occurs to a lesser degree on the surface of trabeculae in epiphyses, such as the site sampled in this report. Though modeling shares the same basic cellular processes with remodeling (osteoclast and osteoblast activity), it appears to be triggered by more vigorous loads[30] and typically yields thickening of the cortical shell via deposition of bone mineral in "drifts"[32-36]. Although we used a biomechanical model to estimate compressive loads in the training protocol[12], we can not non-invasively measure the strains engendered by soleus contraction. We therefore do not know whether soleus loads surpassed the hypothetical threshold for remodeling (in which case routine loads merely "staved off" bone loss) or whether soleus loads were sufficiently vigorous to surpass the hypothetical threshold for modeling (in which case true bone anabolism would occur). Because remodeling is more typical at epiphyseal sites, and because the magnitude of load (1.5 times body weight) is well below loads generated through vigorous volitional activity, we speculate that remodeling was the primary cellular process underlying the observed bone-sparing effect.

Asymmetry of BMD decline

Soleus training longitudinally preserved BMD in the posterior region but not the anterior region of the distal tibia. BMD of the posterior region of the tibia was significantly higher than anterior BMD for the non-SCI subjects (p=0.014). This relationship did not persist for SCI subjects who did not engage in soleus training (p>0.05). The percentage difference in anterior and posterior BMD was higher for the soleus training limbs than for any other subject cohort (Figure 7).

Biomechanics of soleus loads

In designing the soleus training protocol, we aimed to deliver a compressive load of "physiologic" magnitude to the tibia. To ensure uniform administration of load between subjects and over time, we used isometric contractions with the ankle constrained in a neutral joint range. Thus, although the magnitude of compressive load was in the range of physiologic values, the orientation of load directions was highly artificial (i.e., loads followed a single vector and did not oscillate through the bone's cross-section, as would happen with free joint movement). The load created by soleus contraction triggered a bone-sparing effect *only* at the posterior tibia, suggesting: 1) compressive loads were minimal through the anterior portion of the tibia, and/or; 2) bending moments at the posterior tibia were an important osteogenic stimulus. It may be the case that soleus forces placed the posterior aspect of the tibia in compression and the anterior aspect in tension. Although this effect would seem to be more typical for the tibia diaphyseal region, it is possible that the distal epiphysis was exposed to

loads of this type. Previous animal studies of compressive loading have used bone pins[37,38] or external loading devices[39-42] that exerted more symmetric loading of bone as compared to this study. No previous animal studies have examined the bone adaptations to muscle loading in a single vector. Only a handful of studies have examined training effects to bending forces, largely because training with three- or four-point bending elicits undesirable periosteal woven bone formation[43,44]. In sheep radii and ulnae, bending forces enhanced bone remodeling but histological adaptations were similar regardless of whether bone was exposed to tension or to compression[45]. Similarly, mouse tibiae exposed to mediallateral bending showed increased bone formation along both the medial and lateral endocortical surfaces (loaded in tension and compression, respectively)[44]. It appears that the asymmetric adaptations observed in the present study are a unique finding in the literature.

Multifactorial pathology of post-SCI bone loss

Opinions vary widely as to the most culpable factor behind post-SCI bone loss. Some theorists offer a predominantly neurovascular explanation[15,46], a position supported by new evidence for the role of neuropeptides and central neural centers in bone homeostasis[16-21]. The limited effectiveness of some post-SCI bone-protective interventions[3-10] prompted one group to recently state that “Since treatment interventions based on physical activity… have no sufficient positive effects, pharmacological therapy seems to be necessary”[11]. Pharmacologic interventions may well be integral to future bone-protective therapeutic regimens. The present study, however, lends support to the viewpoint that mechanical loading does indeed have much to offer. Perhaps mechanical load triggers bone preservation directly (by regulating osteoblast and osteoclast activity) or perhaps it triggers secondary neural or vascular mechanisms that in turn foster bone adaptation. This issue is fertile ground and the focus of future investigations within our laboratory. In the case of the present study, however, we suspect that the neurovascular milieu of the anterior and posterior halves of the tibia should have been quite similar. (Marrow cavity pressure, for instance, would not be expected to differ between these regions.) In our opinion, the asymmetric nature of tibia adaptations in the present study suggests that soleus mechanical load was the salient stimulus leading to preservation of posterior tibia BMD. Evidence is accumulating that an appropriate, timely dose of mechanical load may be a powerful tool for prevention of post-SCI bone loss.

Translational implications

The study of bone adaptations to muscle loading in the paralyzed human model is sufficiently novel that translational applications remain nascent. This paper and other previous works[12,47] demonstrate the efficacy of muscle loading for attenuating bone decline after SCI. While this strategy appears promising for individuals with recent SCI, individuals with chronic SCI have not demonstrated similar responsiveness[48]. A window of opportunity appears to exist after SCI for interventions that aim to preserve bone integrity[49]. This concept is most amply illustrated by subject SCI 2, who showed the most robust bone-sparing response of the three soleus training subjects. This subject began soleus training only 7 weeks post-SCI, the soonest of any soleus training subject. We have previously suggested that the rapid commencement of soleus loading contributed to this subject's compelling training effect[13].

This report demonstrates that clinical application of electrical muscle stimulation protocols may not be straightforward. If the asymmetric response of bone is typical in other muscle-bone systems, such as at the knee or hip, then future clinical applications may need to load the bone cross-section through multiple vectors. However, even asymmetric maintenance of BMD may be helpful to reduce the risk of fracture, a significant secondary complication after chronic SCI. As neuroscientists advance the possibility for a cure after SCI, it will clearly involve a lengthy rehabilitation process. Accordingly, a non-invasive therapeutic strategy that will sustain skeletal integrity will continue to be an important component of long-term physical restoration

programs for those with SCI. The financial feasibility of long-term daily electrical stimulation training is certainly an issue of concern. Administration of the lion's share of the training dose at home, rather than in the clinic, would greatly minimize the cost and subject burden of such an intervention. Adequate surveillance of subject compliance with dose recommendations will be a critical factor for successful interpretation of potential loading regimens[13].

Summary and conclusions

Long-term training with soleus electrical stimulation preserved BMD in individuals with SCI. Depending on the analysis procedures employed, trabecular BMD was between 27.5% and 40.5% higher in the trained limb than in the untrained limb after 4.5-6 years of training. The bone-sparing effect of soleus stimulation occurred almost entirely in the posterior region of the tibia. In trained limbs, the anterior tibia region BMD did not differ significantly from chronic SCI values, while posterior tibia BMD exceeded chronic SCI values by 64%. This asymmetric adaptation to loading likely reflects the biomechanical stress imposed by isometric soleus loading. Future studies should investigate methods to offer similar bone-sparing effects to multiple skeletal regions across the entire cross-section of bones at risk of fracture after SCI.

Acknowledgements

The authors thank Deanna Frei, RTR, CT, April Miller, RTR, and Daniel Schiferl for their technical expertise during pQCT measurements. This work was supported by an award from the National Institutes of Health (R01-NR 010285-05) and by the Christopher Reeve Paralysis Foundation.

References

1. Lu TW, Taylor SJ, O'Connor JJ, Walker PS. Influence of muscle activity on the forces in the femur: an *in vivo* study. J Biomech 1997;30:1101–6. [PubMed: 9456377]
2. Warden SJ. Breaking the rules for bone adaptation to mechanical loading. J Appl Physiol 2006;100:1441–2. [PubMed: 16614362]
3. Kunkel CF, Scremin AM, Eisenberg B, Garcia JF, Roberts S, Martinez S. Effect of “standing” on spasticity, contracture, and osteoporosis in paralyzed males. Arch Phys Med Rehabil 1993;74:73–8. [PubMed: 8420525]
4. Ben M, Harvey L, Denis S, Glinsky J, Goehl G, Chee S, Herbert RD. Does 12 weeks of regular standing prevent loss of ankle mobility and bone mineral density in people with recent spinal cord injuries? Aust J Physiother 2005;51:251–6. [PubMed: 16321132]
5. Needham-Shropshire BM, Broton JG, Klose KJ, Lebwohl N, Guest RS, Jacobs PL. Evaluation of a training program for persons with SCI paraplegia using the Parastep 1 ambulation system: part Lack of effect on bone mineral density. Arch Phys Med Rehabil 1997;78:799–803. [PubMed: 9344296]
6. Thoumie P, Le Claire G, Beillot J, Dassonville J, Chevalier T, Perrouin-Verbe B, Bedoiseau M, Busnel M, Cormerais A, Courtillon A. Restoration of functional gait in paraplegic patients with the RGO-II hybrid orthosis. A multicenter controlled study. II: Physiological evaluation. Paraplegia 1995;33:654–9. [PubMed: 8584300]
7. Giangregorio LM, Hicks AL, Webber CE, Phillips SM, Craven BC, Bugaresti JM, McCartney N. Body weight supported treadmill training in acute spinal cord injury: impact on muscle and bone. Spinal Cord 2005;43:649–57. [PubMed: 15968302]
8. Leeds EM, Klose KJ, Ganz W, Serafini A, Green BA. Bone mineral density after bicycle ergometry training. Arch Phys Med Rehabil 1990;71:207–9. [PubMed: 2317139]
9. BeDell KK, Scremin AM, Perell KL, Kunkel CF. Effects of functional electrical stimulation-induced lower extremity cycling on bone density of spinal cord-injured patients. Am J Phys Med Rehabil 1996;75:29–34. [PubMed: 8645435]
10. Eser P, de Bruin ED, Telley I, Lechner HE, Knecht H, Stussi E. Effect of electrical stimulation-induced cycling on bone mineral density in spinal cord-injured patients. Eur J Clin Invest 2003;33:412–9. [PubMed: 12713456]

11. Reiter AL, Volk A, Vollmar J, Fromm B, Gerner HJ. Changes of basic bone turnover parameters in short-term and long-term patients with spinal cord injury. Eur Spine J 2007;16:771–6. [PubMed: 16830131]
12. Shields RK, Dudley-Javoroski S. Musculoskeletal plasticity after acute spinal cord injury: effects of long-term neuromuscular electrical stimulation training. J Neurophysiol 2006;95:2380–90. [PubMed: 16407424]
13. Dudley-Javoroski S, Shields RK. Dose estimation and surveillance of mechanical loading interventions for bone loss after spinal cord injury. Phys Ther 2008;88:387–96. [PubMed: 18202080]
14. Maimoun L, Lumbroso S, Paris F, Couret I, Peruchon E, Rouays-Mabit E, Rossi M, Leroux JL, Sultan C. The role of androgens or growth factors in the bone resorption process in recent spinal cord injured patients: a cross-sectional study. Spinal Cord 2006:44791–7.
15. Chantraine A, van Ouwenaller C, Hachen HJ, Schinas P. Intra-medullary pressure and intra-osseous phlebography in paraplegia. Paraplegia 1979;17:391–9. [PubMed: 534112]
16. Hohmann EL, Elde RP, Rysavy JA, Einzig S, Gebhard RL. Innervation of periosteum and bone by sympathetic vasoactive intestinal peptide-containing nerve fibers. Science 1986;232:868–71. [PubMed: 3518059]
17. Imai S, Matsusue Y. Neuronal regulation of bone metabolism and anabolism: calcitonin gene-related peptide-, substance P-, and tyrosine hydroxylase-containing nerves and the bone. Microsc Res Tech 2002;58:61–9. [PubMed: 12203704]
18. Serre CM, Farlay D, Delmas PD, Chenu C. Evidence for a dense and intimate innervation of the bone tissue, including glutamate-containing fibers. Bone 1999;25:623–9. [PubMed: 10593406]
19. Pogoda P, Egermann M, Schnell JC, Priemel M, Schilling AF, Alini M, Schinke T, Rueger JM, Schneider E, Clarke I, Amling M. Leptin inhibits bone formation not only in rodents, but also in sheep. J Bone Miner Res 2006;21:1591–9. [PubMed: 16995814]
20. Takeda S, Elefteriou F, Levasseur R, Liu X, Zhao L, Parker KL, Armstrong D, Ducy P, Karsenty G. Leptin regulates bone formation via the sympathetic nervous system. Cell 2002;111:305–17. [PubMed: 12419242]
21. Patel MS, Elefteriou F. The new field of neuroskeletal biology. Calcif Tissue Int 2007;80:337–47. [PubMed: 17440766]
22. American Spinal Injury Association. International Standards for Neurological Classification of SCI. American Spinal Injury Association; Atlanta, Georgia: 2002.
23. Shields RK, Dudley-Javoroski S, Boaldin KM, Corey TA, Fog DB, Ruen JM. Peripheral quantitative computed tomography: measurement sensitivity in persons with and without spinal cord injury. Arch Phys Med Rehabil 2006;87:1376–81. [PubMed: 17023249]
24. Sale D, Quinlan J, Marsh E, McComas AJ, Belanger AY. Influence of joint position on ankle plantarflexion in humans. J Appl Physiol 1982;52:1636–42. [PubMed: 7107473]
25. Norland Medical Systems I. XCT 2000 Technical Reference. Norland Medical Systems, Inc; White Plains, NY: 2000.
26. Hangartner TN, Gilsanz V. Evaluation of cortical bone by computed tomography. J Bone Miner Res 1996;11:1518–25. [PubMed: 8889852]
27. Eser P, Frotzler A, Zehnder Y, Wick L, Knecht H, Denoth J, Schiessl H. Relationship between the duration of paralysis and bone structure: a pQCT study of spinal cord injured individuals. Bone 2004;34:869–80. [PubMed: 15121019]
28. Eser P, Frotzler A, Zehnder Y, Denoth J. Fracture threshold in the femur and tibia of people with spinal cord injury as determined by peripheral quantitative computed tomography. Arch Phys Med Rehabil 2005;86:498–504. [PubMed: 15759235]
29. Eser P, Schiessl H, Willnecker J. Bone loss and steady state after spinal cord injury: a cross-sectional study using pQCT. Journal of Musculoskelet Neuronal Interact 2004;4:197–8.
30. Frost HM. Bone “mass” and the “mechanostat”: a proposal. Anat Rec 1987;219:1–9. [PubMed: 3688455]
31. Frost HM. The role of changes in mechanical usage set points in the pathogenesis of osteoporosis. J Bone Miner Res 1992;7:253–61. [PubMed: 1585826]
32. Heinonen A, Sievanen H, Kyrolainen H, Perttunen J, Kannus P. Mineral mass, size, and estimated mechanical strength of triple jumpers' lower limb. Bone 2001;29:279–85. [PubMed: 11557373]

33. Nikander R, Sievanen H, Heinonen A, Kannus P. Femoral neck structure in adult female athletes subjected to different loading modalities. J Bone Miner Res 2005;20:520–8. [PubMed: 15746998]
34. Heinonen A, Sievanen H, Kannus P, Oja P, Vuori I. Site-specific skeletal response to long-term weight training seems to be attributable to principal loading modality: a pQCT study of female weightlifters. Calcif Tissue Int 2002;70:469–74. [PubMed: 12016461]
35. Kanehisa H, Fukunaga T. Profiles of musculoskeletal development in limbs of college Olympic weightlifters and wrestlers. Eur J Appl Physiol 1999;79:414–20.
36. Kontulainen S, Sievanen H, Kannus P, Pasanen M, Vuori I. Effect of long-term impact-loading on mass, size, and estimated strength of humerus and radius of female racquet-sports players: a peripheral quantitative computed tomography study between young and old starters and controls. J Bone Miner Res 2003;18:352–9. [PubMed: 12568413]
37. Chow JW, Jagger CJ, Chambers TJ. Characterization of osteogenic response to mechanical stimulation in cancellous bone of rat caudal vertebrae. Am J Physiol 1993;265(2Pt1):E340–7. [PubMed: 8368304]
38. Rubin C, Gross T, Qin YX, Fritton S, Guilak F, McLeod K. Differentiation of the bone-tissue remodeling response to axial and torsional loading in the turkey ulna. J Bone Joint Surg Am 1996;78:1523–33. [PubMed: 8876580]
39. Mosley JR, Lanyon LE. Strain rate as a controlling influence on adaptive modeling in response to dynamic loading of the ulna in growing male rats. Bone 1998;23:313–8. [PubMed: 9763142]
40. Mosley JR, March BM, Lynch J, Lanyon LE. Strain magnitude related changes in whole bone architecture in growing rats. Bone 1997;20:191–8. [PubMed: 9071468]
41. Lee KC, Maxwell A, Lanyon LE. Validation of a technique for studying functional adaptation of the mouse ulna in response to mechanical loading. Bone 2002;31:407–12. [PubMed: 12231414]
42. Robling AG, Hinant FM, Burr DB, Turner CH. Shorter, more frequent mechanical loading sessions enhance bone mass. Med Sci Sports Exerc 2002;34:196–202. [PubMed: 11828225]
43. Torrance AG, Mosley JR, Suswillo RF, Lanyon LE. Noninvasive loading of the rat ulna *in vivo* induces a strain-related modeling response uncomplicated by trauma or periostal pressure. Calcif Tissue Int 1994;54:241–7. [PubMed: 8055374]
44. Robling AG, Burr DB, Turner CH. Partitioning a daily mechanical stimulus into discrete loading bouts improves the osteogenic response to loading. J Bone Miner Res 2000;15:1596–1602. [PubMed: 10934659]
45. O'Connor JA, Lanyon LE, MacFie H. The influence of strain rate on adaptive bone remodelling. J Biomech 1982;15:767–81. [PubMed: 7153230]
46. Chantraine A. Actual concept of osteoporosis in paraplegia. Paraplegia 1978;16:51–8. [PubMed: 733286]
47. Shields RK, Dudley-Javoroski S, Frey Law L. Electrically-induced muscle contractions influence bone density decline after spinal cord injury. Spine 2006;31:548–53. [PubMed: 16508550]
48. Shields RK, Dudley-Javoroski S. Musculoskeletal adaptation in chronic spinal cord injury: effects of long-term soleus electrical stimulation training. Neurorehabil Neural Repair 2006;21:169–79. [PubMed: 17312092]
49. Dudley-Javoroski S, Shields RK. Muscle and bone plasticity after spinal cord injury: review of adaptations to disuse and to electrical muscle stimulation. J Rehabil Res Dev. 2008in press

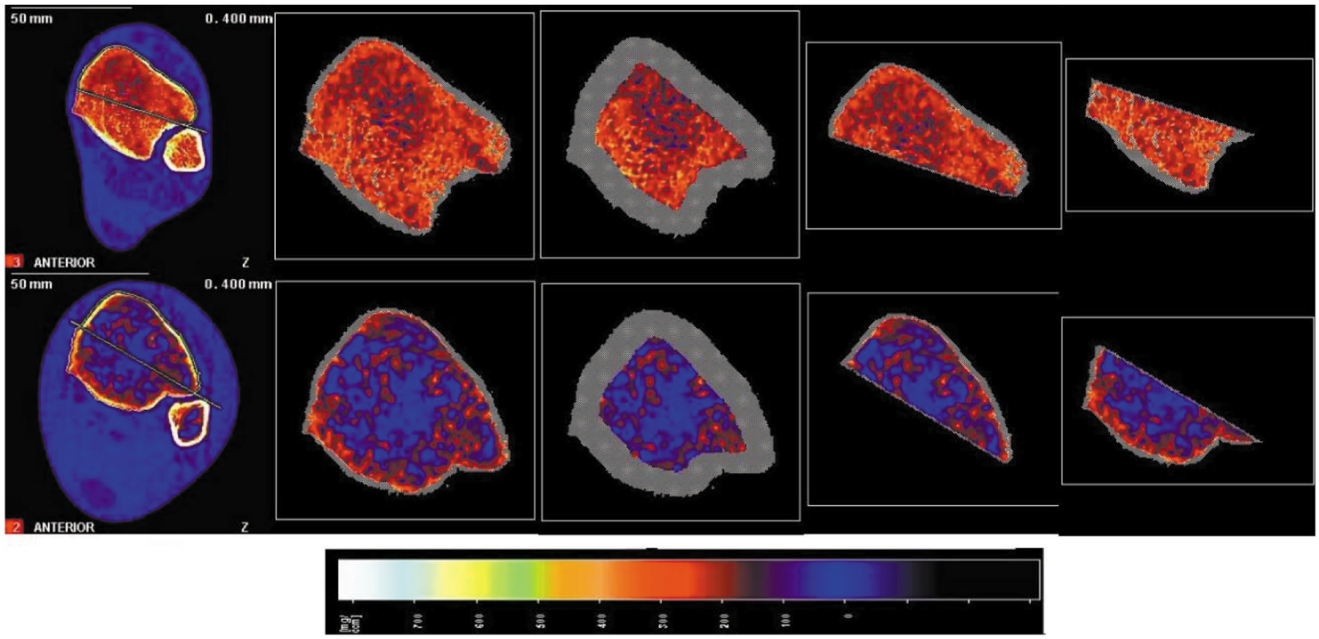

Figure 1.

Representative examples of pQCT scans for a non-SCI (top row) and a chronic SCI subject (bottom row), demonstrating the four modes of analysis. The image is normalized to fat density (0 mg/cm^3). From left to right, the whole image with the line of demarcation in place; the standard analysis of the whole trabecular envelope; the standard analysis of the central 45% of the trabecular envelope; the new analysis of the anterior sub-region; and the new analysis of the posterior sub-region.

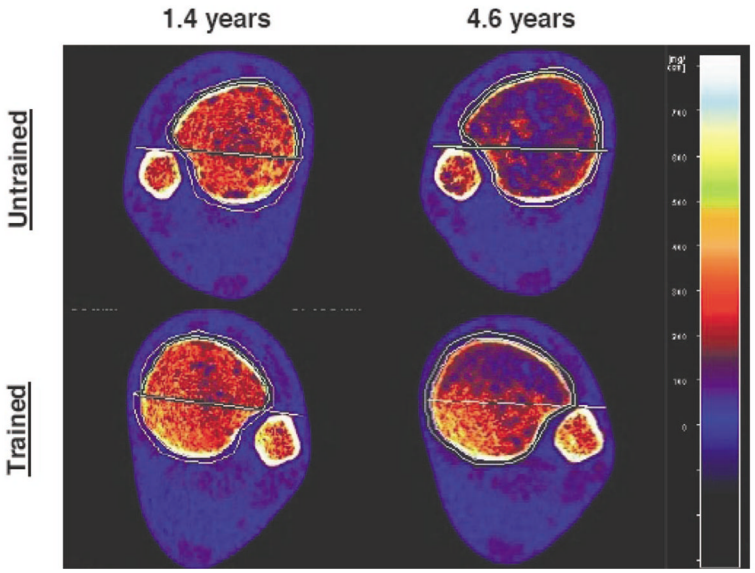

Figure 2.
Longitudinal scan data from both limbs of a single subject who received unilateral soleus muscle training (SCI 2). At this subject's 1.4-year scan time, BMD differed by only 4.7% between limbs. The soleus training effect intensified over time, with the trained limb BMD at 4.6 years exceeding untrained limb BMD by 32.0%.

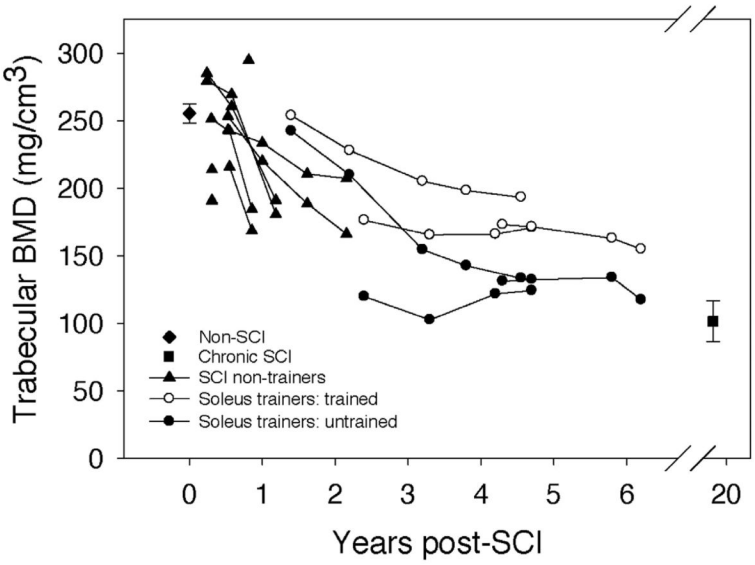

Figure 3.

BMD of the entire 4% tibia site cross-section: "bookend" values of the non-SCI and the chronic SCI cohorts are mean (SE) for all subjects, bilateral limbs. Data from all other subjects are presented longitudinally with each limb shown separately. (The two limbs for a subject on any given scan date share x-axis co-ordinates).

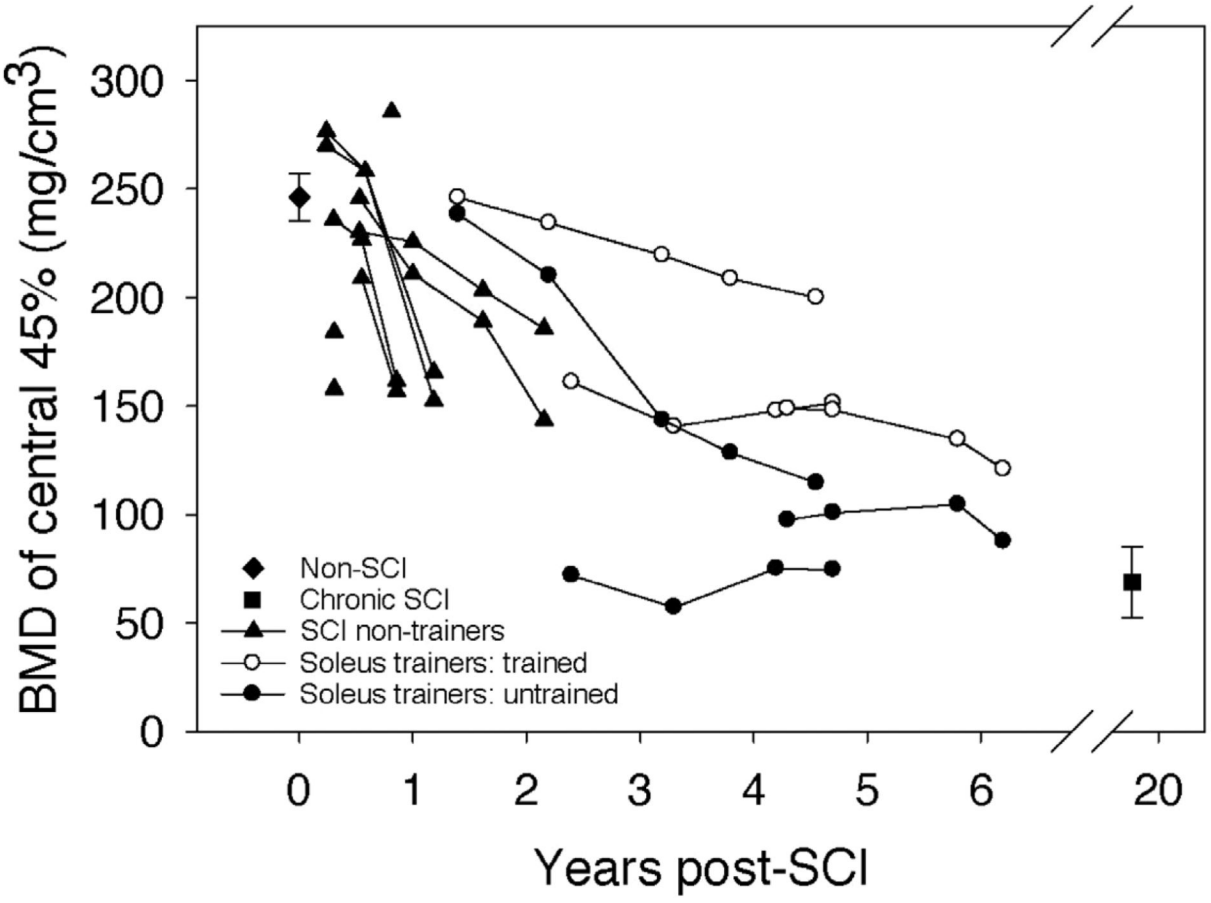

Figure 4.
BMD of the central 45% of the tibia cross-section: "bookend" values of the non-SCI and the chronic SCI cohorts are mean (SE) for all subjects, bilateral limbs. Data from all other subjects are presented longitudinally with each limb shown separately. (The two limbs for a subject on any given scan date share x-axis co-ordinates).

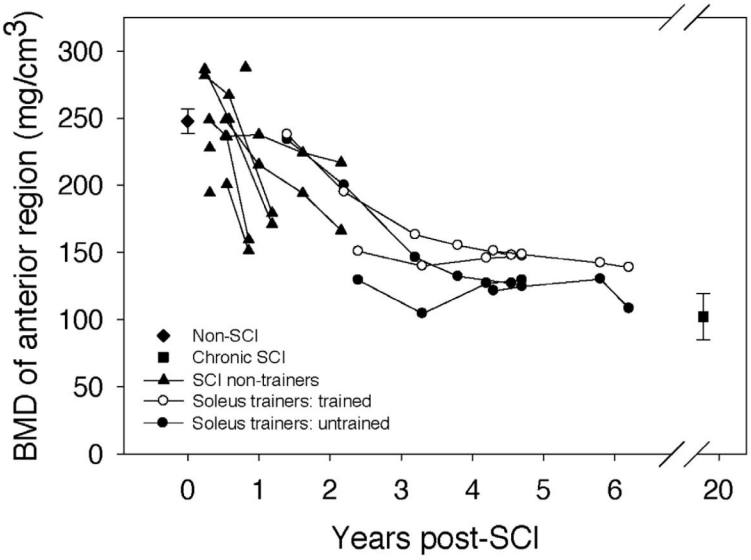

Figure 5.

BMD of the anterior tibia region of interest: "bookend" values of the non-SCI and the chronic SCI cohorts are mean (SE) for all subjects, bilateral limbs. Data from all other subjects are presented longitudinally with each limb shown separately. (The two limbs for a subject on any given scan date share x-axis co-ordinates).

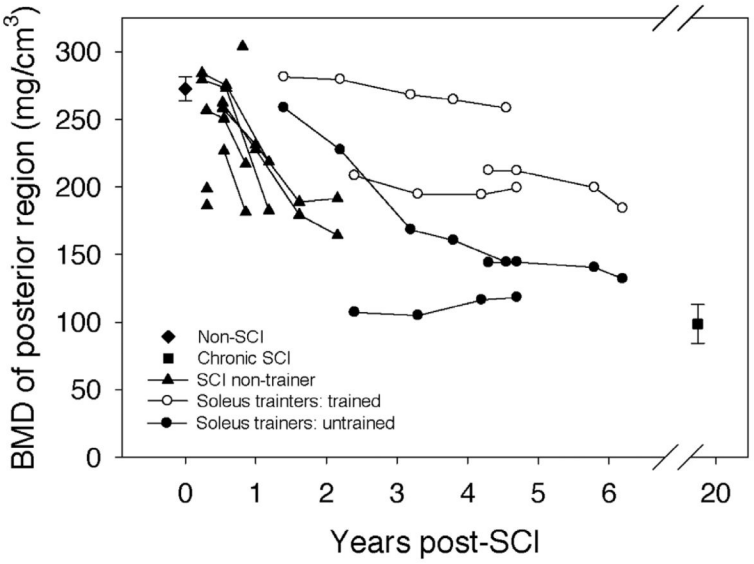

Figure 6.

BMD of the posterior tibia region of interest: "bookend" values of the non-SCI and the chronic SCI cohorts are mean (SE) for all subjects, bilateral limbs. Data from all other subjects are presented longitudinally with each limb shown separately. (The two limbs for a subject on any given scan date share x-axis co-ordinates).

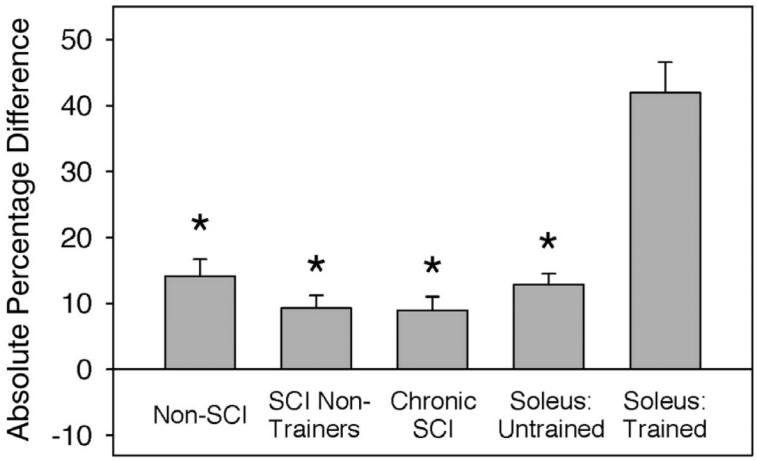

Figure 7.

Absolute difference in anterior and posterior BMD of the tibia, expressed as a percentage of anterior BMD. Right and left limb data are pooled for the non-SCI, SCI non-trainer, and chronic SCI cohorts. “Soleus untrained/trained” refers to the untrained and trained limbs of the soleus training cohort. *=significantly lower than the trained limb of the soleus training cohort ($p<0.05$).

Table 1

Subject demographics.

Subject	Age	SCI level	$ASIA_{22}$ Score	SCI years	Training Participant
SCI 1	28	T4	A	5.2	Y
SCI 2	26	T4	A	4.6	Y
SCI 3	36	T9	A	6.2	Y
SCI 4	39	T8	A	1.6	N
SCI 5	21	T8	A	2.2	N
SCI 6	28	T7	A	0.9	N
SCI 7	49	C6-7	B	0.3	N
SCI 8	22	T11	A	0.8	N
SCI 9	35	C5-6	B	18	N
SCI 10	32	C8	A	18.5	N
SCI 11	46	C5-6	B	22.5	N
SCI 12	72	C5-6	A	18.5	N
NON 1	24	-	-	-	-
NON 2	25	-	-	-	-
NON 3	30	-	-	-	-
NON 4	34	-	-	-	-
NON 5	43	-	-	-	-
NON 6	50	-	-	-	-
NON 7	61	-	-	-	-

SCI and non-SCI subjects are denoted by “SCI” and “NON”, respectively.

Table 2

Anterior and posterior tibia BMD.

	Non-SCI	Chronic SCI	Trained	Untrained
Anterior	247.6†	102.3*	143.0*	129.0*
Posterior	272.7†§	98.5*	203.9*†§	134.1*§

Values are mean BMD in mg/cm^3 for each cohort/region. Trained and Untrained refer to the trained and untrained limbs of the soleus training cohort at the final longitudinal measurement point. Statistical significance is set at p=0.05.

*Significantly lower than non-SCI.

†Significantly higher than chronic SCI.

§Significantly higher than anterior region.